Electronic Supplementary Material (ESI) for Journal of Materials Chemistry C.

Supporting Information for:

Broadband white-light emission from a novel two-dimensional metal halide assembled by Pb-Cl hendecahedrons

Runan Chen,[1] Hao Gu,[2] Han Ying,[1] Jun Yin,[3] Guichuan Xing,[2] and Bin-Bin Cui[1,]*

[1]Advanced Research Institute of Multidisciplinary Science, Beijing Institute of Technology (BIT), Beijing 100081, P. R. China.

[2]Joint Key Laboratory of the Ministry of Education, Institute of Applied Physics and Materials Engineering, University of Macau, Avenida da Universidade, Taipa, Macau 999078, P. R. China.

[3]Advanced Membranes & Porous Materials Center, KAUST Catalysis Center, Division of Physical Science and Engineering, King Abdullah University of Science and Technology, Thuwal 23955-6900, Kingdom of Saudi Arabia. Correspondence and requests for materials should be addressed to B.B.C. (email: cui-chem@bit.edu.cn).

Methods

Materials. Lead(II) chloride ($PbCl_2$, ⩾99.0%), p-Phenylenediamine (⩾99.5%), hydrochloric acid (36-38wt.% in H_2O), anhydrous ether, acetone. The above are all the chemicals that need to be used without further purification.

P-phenylenediamine hydrochloride. Due to the solubility problem of p-phenylenediamine, it is necessary to synthesize the hydrochloride of p-phenylenediamine firstly for synthesizing metal halide single crystals with better purity. These salts were synthesized using a rotary evaporator. Added excess acid to p-phenylenediamine (1.000 g, 9.224 mmol), and sited the condensate temperature to minus 15°C, with the water bath heating temperature to 90°C, and the rotation speed to 60r/min. Distillation was continued under reduced pressure until the corresponding salt product is obtained. Finally, salts were placed in a vacuum drying oven, and the product could be taken out after being stored for about 2 days under vacuum.

Synthesis of 2D (PPD)Pb_2Cl_6 crystal (CCDC 2131056)

With a rotary magnet, dissolved lead chloride (0.060g, 0.216mmol) in 3 ml of hydrochloric acid to an 8 mL bottle, and then added the prepared p-phenylenediamine hydrochloride (0.013 g, 0.072 mmol). Continued heating and stirring it on a heating table at 80°C for 5 hours. Then took out the magnets and the mixture slowly cooled to room temperature to obtain a clear precursor solution. The solution was placed in a larger test tube with 5 ml of anhydrous ether as the antisolvent diffusion, finally sealed the mouth of the test tube and placed it in a constant temperature refrigerator at 2°C. After about 5 days, the poor solvent in the large test tube gradually diffused into the vial. Colorless crystals (PPD)Pb_2Cl_6 will precipitate out at the bottom of the vial. White nearly transparent crystals were isolated from the mother liquor using acetone.

Recrystallization of single crystal materials

(PPD)Pb_2Cl_6 single crystal (0.060g, 0.081 mmol) was dissolved in 5ml HCl solution, and then p-phenylenediamine raw material (0.009 g, 0.083 mmol) was added in equal proportion and stirred at 80°C until the solution was clear and transparent, and then cooled to room temperature to obtain a clear precursor solution. The vial containing solution was placed into a larger test tube with 5 ml of anhydrous ether as the antisolvent diffusion, finally sealed the mouth of the test tube and placed it in

a constant temperature refrigerator at 2°C. After a rest of about 7 days, the poor solvent in the large test tube gradually diffused into the vial. Recrystallized crystals will precipitate out at the bottom of the vial. Nearly transparent crystals were isolated from the mother liquor using acetone.

Single crystal X-ray diffraction (SCXRD). Single crystal x-ray diffraction datas of $(PPD)Pb_2Cl_6$ were collected using a Bruker APEX-II CCD diffractometer with graphite-monochromated Mo Kα radiation. $(PPD)Pb_2Cl_6$ single crystal were kept at a steady T = 150 K during data collection. A complete sphere $(PPD)Pb_2Cl_6$ data was collected using Φ and ω scans with 1°frame widths to a resolution of approximately 0.83 Å, equivalent to $2\theta \approx 55°$, $(PPD)Pb_2Cl_6$ approximately 0.83 Å, equivalent to $2\theta \approx 55°$. Crystal structure of $(PPD)Pb_2Cl_6$ were solved with the ShelXT 2018/2 (Sheldrick, 2018) solution program using dual methods and by using Olex2 as the graphical interface. The model was refined with ShelXL 2018/3 (Sheldrick, 2015) using full matrix least squares minimisation on $\boldsymbol{F^2}$. All non-hydrogen atoms were refined anisotropically. Hydrogen atom positions were calculated geometrically and refined using the riding model. Hydrogen atom positions were calculated geometrically and refined using the riding model.

Powder X-ray diffraction (PXRD). The PXRD analysis was performed on Panalytical X'PERT Pro Powder X-Ray Diffractometer using Copper X-ray tube (standard) radiation at a voltage of 40 kV and 40 mA, and X'Celerator RTMS detector. The diffraction pattern was scanned over the angular range of 5-65 degree (2θ) with a step size of 0.02, at room temperature. Simulated powder patterns were calculated by Mercury software using the crystallographic information file (CIF) from single-crystal x-ray experiment.

Optical measurements. Absorption spectra (with a 1 nm interval) scanning through synchronous of bulk 2D $(PPD)Pb_2Cl_6$ crystals were collected on a FLS980 spectrofluorometer (Edinburgh Instruments) incorporating with an integrating sphere at 298 K. Quartz plates were used in spectroscopic measurements. The absolute photoluminescence quantum efficiencies (PLQEs) were acquired on powders by a FLS980 spectrofluorometer coupled to an integrating sphere. Samples were excited by input light from a 450 W Xe lamp passed through a single grating Czerny-Turner monochromator. The spectra of the emitted light and any unabsorbed excitation light were measured

using a Princeton Instruments Spectra Pro 500i spectrograph fiber-coupled to the sphere. Time-Resolved Emission data were collected at room temperature using time-correlated single photon counting on a FLS1000/FS5 Fluorometer. Samples were excited with 300 nm pulsed diode lasers. (PPD)Pb_2Cl_6 was selected to detect the fluorescence lifetime at 500 nm. The average lifetime was obtained from the tri-exponential decays according to equation： $\tau_{ave} = \sum A_i\tau_i^2 \Big| \sum A_i\tau_i$, $i = 1,2,3$. Where τ_i represents the decay time and A_i represents the amplitude of each component.

Photoluminescence at different temperatures were measured on a PL at different temperatures were measured on a FLS980 spectrofluorometer attached to a OptistatDN cryostat filled with liquid nitrogen. Steady-state photoluminescence spectra of the crystals were obtained at 298 K on a Varian Cary Eclipse Fluorescence spectrophotometer.

Thermogravimetry Analysis (TGA). TGA was carried out using a TA instruments SDT: simultaneous DSC & TGA system of Q600 model. The samples were heated from room temperature (around 22 ℃) to 900 ℃ at a rate of 10 ℃·min^{-1}, under an nitrogen flux of 100 mL·min^{-1}.

Raman spectrum. The measurements were performed upon single crystals of perovskite, using a in Via Raman Microscope Renishaw micro-Raman confocal microscope (with a 10 x objective and a 532 nm excitation wavelength). All measurements were performed in air.

IR spectrum. The analysis was performed by Nicolet IS10 FT-IR spectrometer. The wave number range is 400-4000 cm^{-1}, the spectrometer resolution is 4 cm^{-1}, the SIGNal-to-noise ratio is 5000:1, and 64 scans.

Density Functional Theory (DFT) Calculations.

We performed DFT calculations for 2D hybrid perovskite crystals (PPD)Pb_2Cl_6, by using the generalized gradient approximation (GGA) together with the Perdew-Burke-Ernzerhof (PBE) functional in the Vienna ab initio simulation package (VASP). Startingfrom the experimental lattice parameters for (PPD)Pb_2Cl_6 with the space group of C2/C, both the cell parameters and atomic positions for the two crystal structures were further relaxed until the total Hellmann-Feynman forces on each atom were less than 0.01 eV/Å. Uniform Brillouin zone grids for a 6×2×1 k-mesh were used for (PPD)Pb_2Cl_6 bulk, and a 2×2×1 k-mesh was used for 1×3×1 (PPD)Pb_2Cl_6 supercells.

Table S1. Single crystal X-ray diffraction data of 2D bulk single crystals.

Identification code	$(PPD)Pb_2Cl_6$
Empirical formula	$C_3H_5Cl_3NPb$
Formula weight	368.62
Temperature/K	150.0
Crystal system	monoclinic
Space group	$P2_1/c$
a/Å	13.7001(6)
b/Å	7.8192(3)
c/Å	7.4372(3)
α/°	90
β/°	105.274(2)
γ/°	90
Volume/$Å^3$	768.56(5)
Z	4
Density(calc)g/cm^3	3.186
μ/mm^{-1}	22.895
F(000)	652.0
Crystal size/mm^3	0.20 × 0.15 × 0.10
Radiation	MoKα (λ = 0.71073)
2Θ range for data collection/°	3.027 to 26.381
h,k,lmax	17, 9, 9
Reflections collected	5671
Measured Refl's.	11897
Indep't Refl's	1573
Refl's I≥2 σ(I)	1394
Final R indexes [I>=2σ (I)]	R_1 = 0.0370, wR_2 = 0.1200

Final R indexes [all data]	R_1 = 0.0408, wR_2 = 0.1218
Largest diff. peak/hole / e Å^{-3}	2.797/-2.197

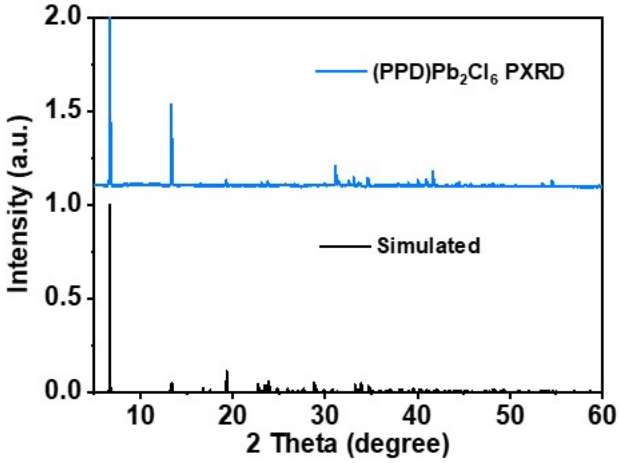

Figure S1. Powder X-ray diffraction (PXRD) spectrum of (PPD)Pb_2Cl_6 bulk crystals, as well as the single crystals based simulated results.

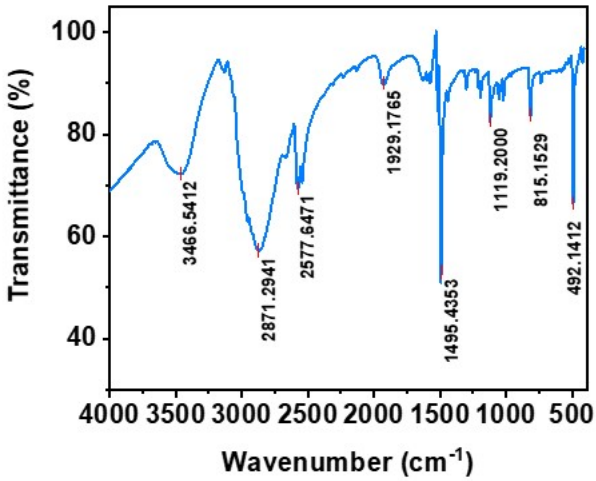

Figure S2. Infrared spectroscopy (IR) analysis of (PPD)Pb_2Cl_6 crystals at room temperature.

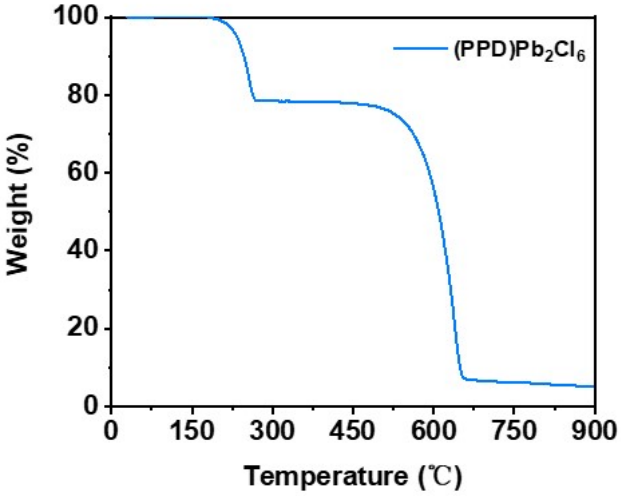

Figure S3. Thermal analysis. TGA characterization of $(PPD)Pb_2Cl_6$.

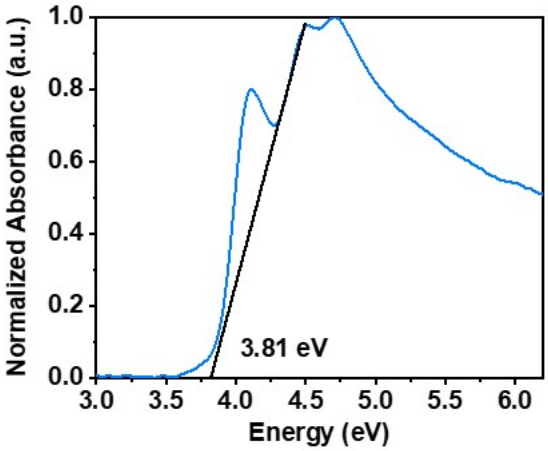

Figure S4. Evaluation of the band gaps from the absorption spectra for $(PPD)Pb_2Cl_6$.

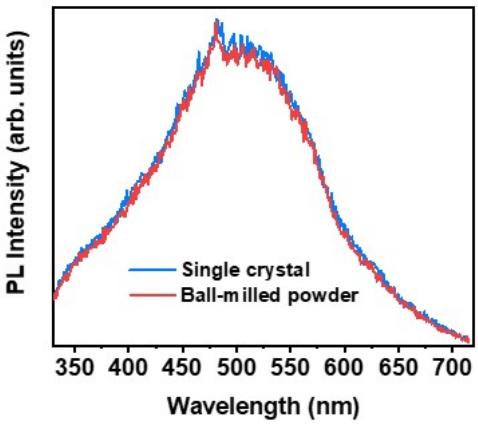

Figure S5. Photoluminescence from single crystals and ball-milled powders of $(PPD)Pb_2Cl_6$.

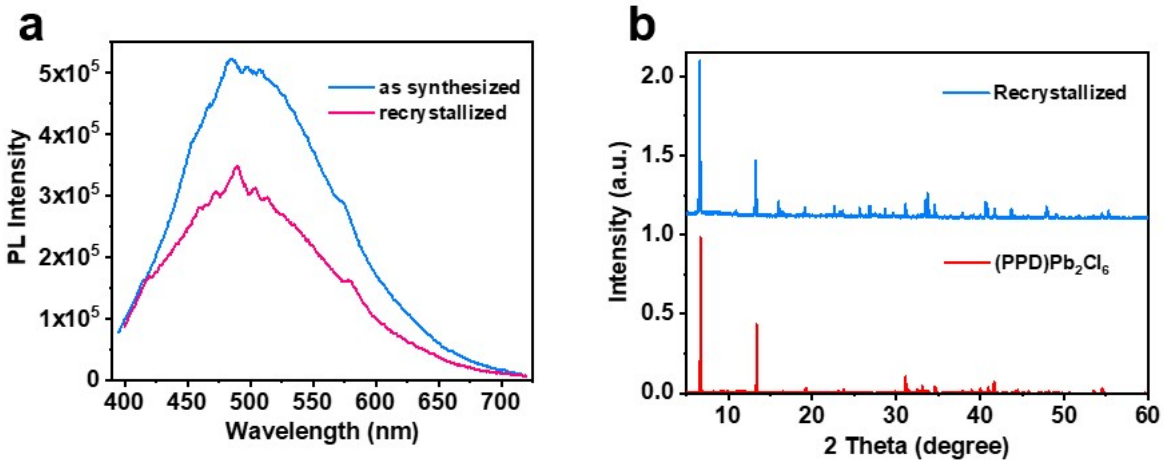

Figure S6. (a) Photoluminescence from single crystals and recrystallized powders of $(PPD)Pb_2Cl_6$; (b) Powder X-ray diffraction (PXRD) spectrum of recrystallized powders of $(PPD)Pb_2Cl_6$, as well as the single crystals based simulated results.

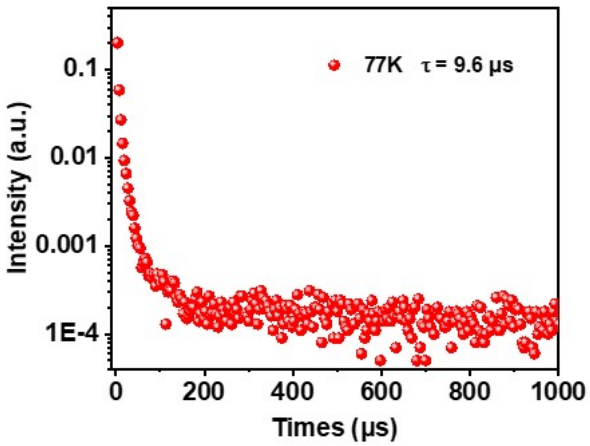

Figure S7. Time-resolved PL decay of the bulk crystals $(PPD)Pb_2Cl_6$ at 77K.

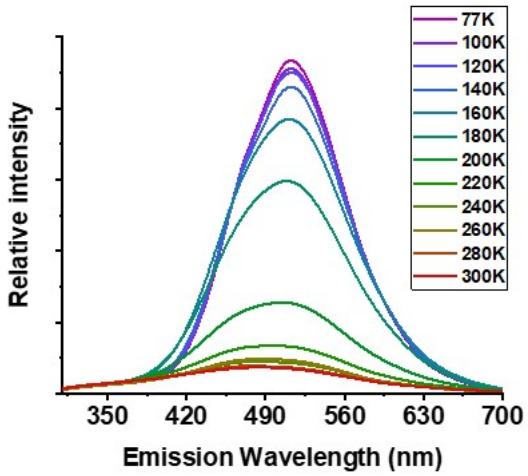

Figure S8. Evolution of PL emission for the chloride compound $(PPD)Pb_2Cl_6$ with temperature.

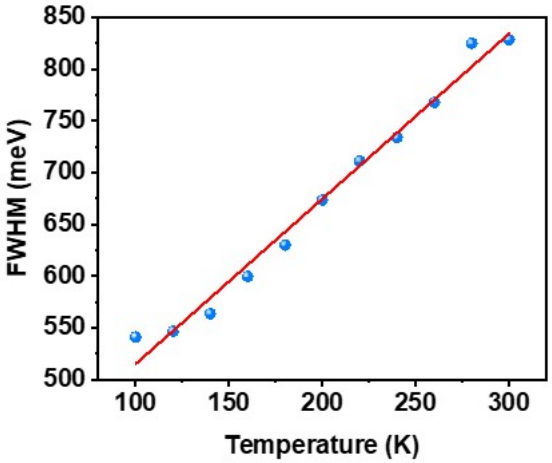

Figure S9. Full width at half-maximum (FWHM) of the $(PPD)Pb_2Cl_6$ follows a linear trend with increasing temperature (FWHM at each temperature is represented by a circle).

Table S2. Summary of reported 2D perovskites with broadband emission

Dimension	Formula	Peak /nm	FWHM /nm	PLQY /%	Ref.
110-2D	$(C_6H_{13}N_3)[PbCl_4]$	573	220	< 1	[1]
100-2D	$(C_6H_5C_2H_4NH_3)_2PbCl_4$	~ 550	~ 230	< 1	[2]
100- 2D	(EDBE)$[PbCl_4]$	538	208	2	[3]
100- 2D	[DMPDA]$PbCl_4$	443	104	4.9	[4]
100-2D	(γ-Methoxy propyl amine)$_2PbBr_4$	~ 470	~ 200	6.85	[5]
100-2D	$(C_7H_7N_2)_2PbCl_4$	500	245	13.31	[6]
100-2D	$(PPD)Pb_2Cl_6$	500	177	17.17	This work

Table S3. Each undecahedron of (PPD)Pb_2Cl_6 has the same bond angle, and its bond angles data are shown in the table below.

Cl(x)–Pb–Cl(y)	bond angles (deg)
phi(Cl2a-Pb1-Cl2b)	78.974
phi(Cl2b-Pb1-Cl3a)	81.396
phi(Cl3a-Pb1-Cl2c)	71.912
phi(Cl2c-Pb1-Cl2d)	71.233
phi(Cl2d-Pb1-Cl3c)	80.159
phi(Cl3c-Pb1-Cl3b)	90.429
phi(Cl3b-Pb1-Cl4a)	78.126
phi(Cl4a-Pb1-Cl2a)	81.992
phi(Cl2a-Pb1-Cl3a)	63.747
phi(Cl2a-Pb1-Cl3b)	74.559
phi(Cl2a-Pb1-Cl2d)	105.247
phi(Cl2b-Pb1-Cl2c)	78.316
phi(Cl2b-Pb1-Cl3c)	109.591

phi(Cl2b-Pb1-Cl4a)	81.045
phi(Cl2c-Pb1-Cl3c)	68.539
phi(Cl3a-Pb1-Cl2d)	67.896
phi(Cl3a-Pb1-Cl3b)	101.926
phi(Cl2d-Pb1-Cl3b)	63.899
phi(Cl3c-Pb1-Cl4a)	80.578

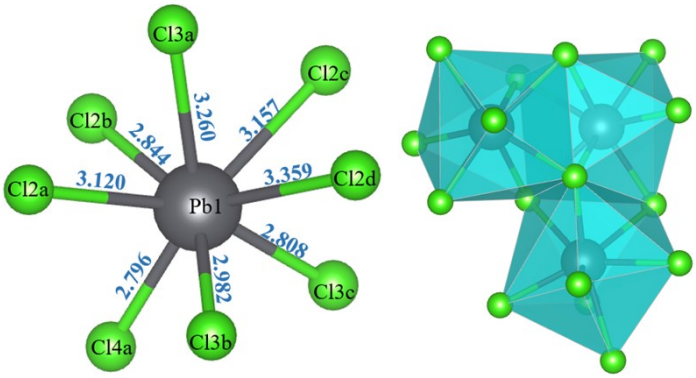

Figure S10. Structural model of chains and bond length for (PPD)Pb_2Cl_6. Each of the hendecahedrons exists as a coplanarity, with one parallelogram face and two triangular faces.

Table S4. Raman Modes for range 50 to 300 cm^{-1}.

Range (cm^{-1})	Mode	Mode position (cm^{-1})	FWHM (cm^{-1})	Intensity x10^4
50-110	(Cl-Pb-Cl) Bending mode ~64cm^{-1}	61	24	0.8591
	(Pb-Cl) stretching mode ~80 to 100cm^{-1}	92	37	2.0774
		105	30	0.7156
110-300	Weak band due to organic cation liberation from deformed Pb-Cl inorganic	169	48	1.3564

	cage ~ 150 to 200cm^{-1}	215	135	0.5060

Reference

1. Z. Wu, C. Ji, Z. Sun, S. Wang, S. Zhao, W. Zhang, L. Li and J. Luo, *J. Mater. Chem. C*, 2018, **6**, 1171-1175.
2. K. Thirumal, W. K. Chong, W. Xie, R. Ganguly, S. K. Muduli, M. Sherburne, M. Asta, S. Mhaisalkar, T. C. Sum and H. S. Soo, *Chem. Mater.*, 2017, **29**, 3947-3953.
3. E. R. Dohner, A. Jaffe, L. R. Bradshaw and H. I. Karunadasa, *J. Am. Chem. Soc.*, 2014, **136**, 13154-13157.
4. C. Q. Jing, J. Wang, H. F. Zhao, W. X. Chu, Y. Yuan, Z. Wang, M. F. Han, T. Xu, J. Q. Zhao and X. W. Lei, *Chem.–Eur. J.*, 2020, **26**, 10307-10313.
5. Y. Li, C. Ji, L. Li, S. Wang, S. Han, Y. Peng, S. Zhang and J. Luo, *Inorg. Chem. Front.*, 2021, **8**, 2119-2124.
6. Y. Han, J. Yin, G. Cao, Z. Yin, Y. Dong, R. Chen, Y. Zhang, N. Li, S. Jin, O. F. Mohammed, B.-B. Cui and Q. Chen, *ACS Energy Lett.*, 2021, **7**, 453-460.